Pis'ma v ZhETF, vol. 84, iss. 10, pp. 631 – 635 

# Unitarity constraints for DIS off nuclei: predictions for electron-ion colliders

*N. N. Nikolaev*[+*], *W. Schäfer*[△], *B. G. Zakharov*[*], *V. R. Zoller*[□]

[+] *IKP(Theorie), FZ Jülich, Jülich, Germany*

[*] *L.D. Landau Institute for Theoretical Physics RAS, 119334 Moscow, Russia*

[△] *Institute of Nuclear Physics PAN, PL-31-342 Cracow, Poland*

[□] *Institute for Theoretical and Experimental Physics, 117218 Moscow, Russia*

Submitted 25 October 2006

Future electron-ion colliders (eIC) will focus on the unitarity properties of deep inelastic scattering (DIS) in the limit of strong nuclear absorption. Strong nuclear shadowing and a large abundance of coherent diffraction are the most striking consequences of unitarity, and here we report quantitative predictions for these effects in the kinematical range of the planned eIC.

PACS: 12.38.–t, 13.60.Hb

**1. Introduction.** In deep-inelastic scattering off nuclei at the Bjorken variable

$$x \ll x_A = \frac{1}{m_N R_A} = 0.15 A^{-1/3}, \qquad (1)$$

where $R_A$ is the radius of the target nucleus of mass number $A$ and $m_N$ is the nucleon mass, unitarity driven nuclear shadowing (NS) becomes important [1 – 3]. It comes along with the large-rapidity-gap coherent diffractive DIS (LRG DIS) when the target nucleus remains in the ground state. For strongly absorptive nuclei the unitarity condition was shown to imply a paradoxically large, $\sim 50\%$, fraction of LRG DIS [4] (for the experimental confirmation of LRG DIS off nuclei see [5], similar calculations were reported in the recent Ref. [6]). It is precisely the s-channel unitarity condition which controls the interplay of the virtual and real pQCD radiative corrections in the small-$x$ evolution of different nuclear observables [7]. In this communication we report quantitative predictions for the small-$x$ evolution of NS and LRG DIS for the energy range of future eIC [8] which will test the unitarity properties of hard scattering processes under strong nuclear absorption (saturation) .

**2. First iteration of the LL($1/x$) evolution for nuclear cross sections.** We base our work on the color dipole (CD) approach to the Leading Log($1/x$) (LL($1/x$)), or BFKL [9], evolution of DIS [10, 11]. For nuclear targets a complete resummation of LL($1/x$) effects is as yet lacking, the Double Leading Log [12], large-$N_c$ Color Glass Condensate [2] and the fan diagram resummation [13] approximations were considered in the literature ( for the review see [14], the dominance of fan diagrams was questioned, though [15]). Our point is that at energies of the planned eIC [8], the $x$-dependence of NS and LRG DIS is practically exhausted by the first CD LL($1/x$) iteration which is calculable exactly without invoking the large-$N_c$ approximation [2, 3]. Indeed, the first CD LL($1/x$) iteration dominates in the $x$ region

$$\xi = \log \frac{x_0}{x} \lesssim \frac{1}{\Delta_{\rm eff}}, \qquad (2)$$

where $\Delta_{\rm eff} \simeq 0.1 - 0.2$ is the exponent of the local $x$-dependence of the proton structure function, $F_{2p} \propto \propto x^{-\Delta_{\rm eff}}$ [16].

When viewed in the laboratory frame, NS derives from the coherent interaction of $q\bar{q}, q\bar{q}g, ...$ states. To the required accuracy, the Fock state expansion of the physical photon $|\gamma^*\rangle$ reads $|\gamma^*\rangle = \sqrt{Z_g}\Psi_{q\bar{q}}|q\bar{q}\rangle + + \Phi_{q\bar{q}g}|q\bar{q}g\rangle$,where $\Psi_{q\bar{q}}$ and $\Phi_{q\bar{q}g}$ are the light-cone wave functions (WF's) of the $q\bar{q}$ and $q\bar{q}g$ states, $\sqrt{Z_g}$ is the renormalization of the $q\bar{q}$ state by the virtual radiative corrections for the $q\bar{q}g$ state. For soft gluons the 3-parton WF takes the factorized form $\Phi_{q\bar{q}g} = \Psi_{q\bar{q}}\{\Psi_{qg} - \Psi_{\bar{q}g}\}$ [10, 11]. The nuclear coherency condition reads [1]

$$x/\beta \lesssim x_A, \qquad (3)$$

where $x = Q^2/2m_N\nu$ is the Bjorken variable, $\nu$ is the energy of the photon, $M$ is the invariant mass of the multiparton Fock state and $\beta = Q^2/(M^2 + Q^2)$.

In the CD BFKL-Regge phenomenology of DIS one usually formulates the boundary condition at $x = x_0 = = 0.03$ [17]. For extremely heavy nuclei $x_A \ll x_0$ and the LL($1/x$) evolution starts at $x = x_A$ with the boundary

condition formulated in terms of the free-nucleon quantities LL$(1/x)$-evolved from $x_0$ down to $x_A$. At small $x$ satisfying the condition (3) the color dipoles $\{\mathbf{r}_n\}$ in the multiparton state are conserved in the interaction process. At the boundary $x = x_A$ and for $A \gg 1$, the nuclear S-matrices equal [18, 19]

$$\mathsf{S}_n(x_A, \mathbf{b}, \{\mathbf{r}\}_n) = \exp\left[-\frac{1}{2}\sigma_n(x_A, \{\mathbf{r}\}_n)T(\mathbf{b})\right], \quad (4)$$

where $\sigma_n(x_A, \{\mathbf{r}\}_n)$ is the free-nucleon CD cross section for the $n$-parton state, and [20]

$$\sigma_{2,A}(x_A, \mathbf{r}) = 2\int d^2\mathbf{b}[1 - \mathsf{S}_2(x_A, \mathbf{b}, \mathbf{r})]. \quad (5)$$

Here $T(\mathbf{b}) = \int_{-\infty}^{+\infty} dz n_A(\sqrt{z^2 + \mathbf{b}^2})$, is the optical thickness of a nucleus at an impact parameter $\mathbf{b}$, the nuclear matter density $n_A(\mathbf{r})$ is normalized as $\int d^3\mathbf{r} n(\mathbf{r}) = A$.

A quite common extension of Eq.(5) to $x \ll x_A$ with the BFKL-evolved $\sigma_2(x, \mathbf{r})$ is completely unwarranted. Instead one must evolve the nuclear S-matrix. Specifically, after the gluon variables have been properly integrated out, the effect of the extra gluon in the Fock state expansion for the incident photon boils down to the renormalization of the S-matrix and nuclear cross section for the $q\bar{q}$ CD [10, 11, 7]:

$$\frac{\partial \mathsf{S}_2(x, \mathbf{r}; \mathbf{b})}{\partial \xi} =$$
$$= \int d^2\boldsymbol{\rho}|\psi(\boldsymbol{\rho}) - \psi(\boldsymbol{\rho} + \mathbf{r})|^2\Big[\mathsf{S}_3(x, \boldsymbol{\rho}, \mathbf{r}; \mathbf{b}) - \mathsf{S}_2(x, \mathbf{r}; \mathbf{b})\Big],$$

$$\sigma_A(x, \mathbf{r}) = \sigma_{2,A}(x_A, \mathbf{r}) + \sigma_A^{(1)}(x, \mathbf{r}),$$

$$\sigma_A^{(1)}(x, \mathbf{r}) =$$
$$= 2\log\left(\frac{x_A}{x}\right)\int d^2\mathbf{b}\int d^2\boldsymbol{\rho}|\psi(\boldsymbol{\rho}) - \psi(\boldsymbol{\rho} + \mathbf{r})|^2 \times \quad (6)$$
$$\times \Big[\mathsf{S}_2(x_A, \mathbf{r}; \mathbf{b}) - \mathsf{S}_3(x_A, \boldsymbol{\rho}, \mathbf{r}; \mathbf{b})\Big],$$

$$\sigma_3(x, \mathbf{r}, \boldsymbol{\rho}) =$$
$$= \frac{N_c^2}{N_c^2 - 1}\Big[\sigma_2(x, \boldsymbol{\rho}) + \sigma_2(x, \boldsymbol{\rho} + \mathbf{r})\Big] - \frac{1}{N_c^2 - 1}\sigma_2(x, \mathbf{r}),$$

where $\rho$ is the $qg$ dipole and

$$\psi(\boldsymbol{\rho}) = \frac{\sqrt{C_F\alpha_S}}{\pi} \cdot \frac{\boldsymbol{\rho}}{\rho^2} \cdot \frac{\rho}{R_c}K_1\left(\frac{\rho}{R_c}\right) \quad (7)$$

is the radial WF of the $qg$ state with the Debye screening of infrared gluons [10, 11]. The virtual photoabsorption cross section is an expectation value $\sigma_A(x, Q^2) = \langle q\bar{q}|\sigma_A(x, \mathbf{r})|q\bar{q}\rangle$.

The shadowing ratio $R_A(x, Q^2)$, decomposed into the $q\bar{q}$ and $q\bar{q}g$ contributions, equals

$$R_A(x, Q^2) = \frac{\sigma_A(x, Q^2)}{A\sigma_N(x, Q^2)} =$$
$$= 1 - \frac{A\sigma_{2,N}(x_A, Q^2) - \sigma_{2,A}(x_A, Q^2)}{A\sigma_N(x, Q^2)} -$$
$$- \log\left(\frac{x_A}{x}\right)\frac{A\sigma_N^{(1)}(x_A, Q^2) - \sigma_A^{(1)}(x_A, Q^2)}{A\sigma_N(x, Q^2)}, \quad (8)$$

where

$$\sigma_N(x, Q^2) = \sigma_{2,N}(x_A, Q^2) + \log(x_A/x)\sigma_N^{(1)}(x_A, Q^2)$$

is the LL$(1/x)$-evolved free-nucleon cross section. Our interest is in the well evolved shadowing at $x \ll x_A$, the onset of NS at $x \gtrsim x_A$ must be treated within the light-cone Green function technique [12, 21], here we show only the gross features of the large-$x$ suppression of NS following the prescriptions from Refs. [20, 22] and the $\beta$-dependence of LRG DIS as predicted in [23] and confirmed in the HERA experiments [24]. We use the free-nucleon CD cross section tested against the experimental data from HERA, it is described in the Appendix. The nuclear density parameters are taken from the compilation [25]. In Fig.1 we compare the predictions from

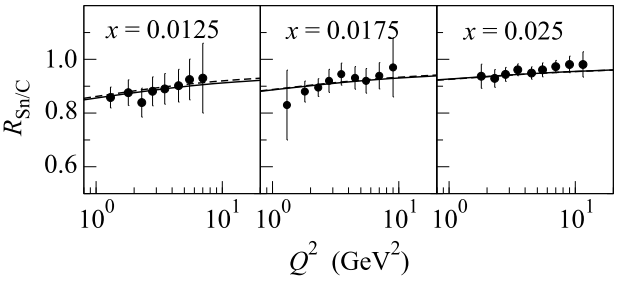


Fig.1. The predictions form CD LL$(1/x)$ evolution vs. the NMC data on the shadowing ratio $R_{\mathrm{Sn/C}}$ [26]. The solid lines represent the full shadowing from the $q\bar{q}$ and $q\bar{q}g$ Fock states, while the dashed lines show a shadowing at the $q\bar{q}$ level, see also a caption to Fig.3

the first LL$(1/x)$ iteration with the NMC data [26] on the ratio of $R_{\mathrm{Sn/C}}(x, Q^2) = R_{\mathrm{Sn}}(x, Q^2)/R_{\mathrm{C}}(x, Q^2)$. The results for $R_{\mathrm{C/D}}$ [27] and $R_{\mathrm{Ca/C}}$ [28] are shown in Fig.2. The agreement with the experimental data is good, but in a limited region of $x, Q^2$ the contribution from the shadowing of the $q\bar{q}g$ Fock states is still small. A much broader range of $x$ and $Q^2$ can be covered at eIC [8], and in Fig.3 we show our predictions for $R_A(x, Q^2)$ at eIC.

**3. LL$(1/x)$ evolution for LRG DIS.** The LL$(1/x)$ evolution of fully inclusive forward LRG DIS

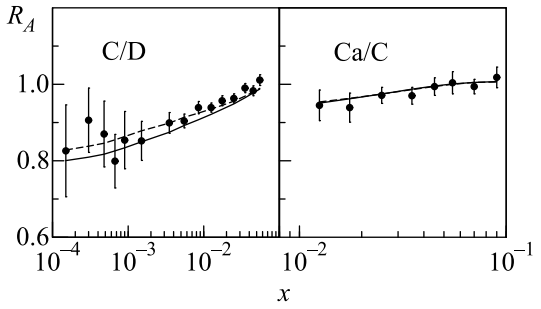


Fig.2. The same as in Fig.1 for the NMC data on the shadowing ratio $R_{\rm C/D}$ [27] and $R_{\rm Ca/C}$ [28] as a function of two correlated variables $x$ and $Q^2$ (for details of $x-Q^2$ correspondence see [27, 28])

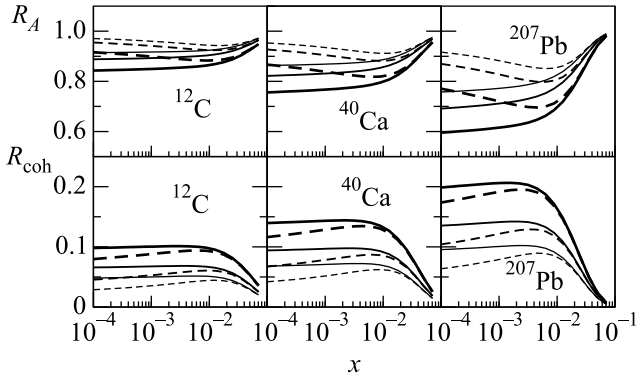


Fig.3. The upper panels: predictions from CD LL($1/x$) evolution for NS ratio $R_A$ for C, Ca and Pb nuclei as a function of $x$ at $Q^2 = 1, 5, 20$ GeV$^2$, the bottom to top curves, respectively. The solid lines show the combined NS (8) from the $q\bar{q}$ and $q\bar{q}g$ Fock states of the photon, while the dashed lines represent NS at the $q\bar{q}$ level, i.e., the term $R_{2,A} = 1 - [A\sigma_{2,N}(x_A, Q^2) - \sigma_{2,A}(x_A, Q^2)]/A\sigma_N(x)$ in the expansion (8). The lower panels: the same as above for the fraction of DIS which is LRG coherent diffraction, $R_{coh}$. Dashed lines represent the contribution from the low-mass $q\bar{q}$ excitations, $\sigma_A^{LM}$, the sum of the low-mass and 3$\mathbb{P}$ high-mass terms is shown by solid lines

off a free nucleon, starting from $x_{\mathbb{P}} = x_0$, has the Fock state expansion [23, 11]

$$\left.\frac{d\sigma_N^D(x,x_0)}{dt}\right|_{t=0} = \frac{1}{16\pi}\left[\langle q\bar{q}|\sigma_2^2(x_0)|q\bar{q}\rangle + \right.$$
$$\left. + \langle q\bar{q}g|\sigma_3^2(x_0) - \sigma_2^2(x_0)|q\bar{q}g\rangle + ...\right], \qquad (9)$$

where $t$ is the $(p,p')$ momentum transfer squared. Upon the integration over the gluon momentum the $q\bar{q}g$ term gives rise to the LL($1/x$) evolution of LRG DIS. Its decomposition [29]

$$\sigma_3^2(x_0) - \sigma_2^2(x_0) = [\sigma_3(x_0) - \sigma_2(x_0)]^2 + $$
$$+ 2\sigma_2(x_0)(\sigma_3(x_0) - \sigma_2(x_0)) \qquad (10)$$

splits the LL($1/x$) evolution into the real production of high-mass (triple-pomeron, 3$\mathbb{P}$) states governed by $[\sigma_3(x_0) - \sigma_2(x_0)]^2$ and the virtual pQCD radiative correction to the Born excitation of low-mass, $M^2 \sim Q^2$, states described by the first term of eq.(10).

For heavy nuclei we consider coherent diffractive DIS per unit area in the impact parameter space, $d\sigma_A^D(x,x_0)/d^2\mathbf{b}$ with the boundary $x_0 = x_A$. At fixed $x \ll x_A$, the small-mass $q\bar{q}$ diffraction enters at $x_{\mathbb{P}} \approx x$, while the small-$x$ evolution of the high-mass diffraction starts with the rapidity gap variable $x_{\mathbb{P}} = x_A$. To the LL($1/x$) approximation, integrating out the gluon variables, one can cast it in the color dipole form [29] $d\sigma_A^D(x,x_A,\mathbf{b})/d^2\mathbf{b} = \langle q\bar{q}|\Sigma_A^D(x,x_A,\mathbf{b},\mathbf{r})|q\bar{q}\rangle$, where, with certain reservations [30], one can dub $\Sigma_A^D(x,x_A,\mathbf{b},\mathbf{r})$ a CD cross section for the pomeron target. Extending the decomposition (10) to nuclear targets, for the high-mass excitations, i.e., 3$\mathbb{P}$ at $x \ll x_A$, one finds [29]

$$\frac{d\sigma_A^{3\mathbb{P}}(x,x_A,\mathbf{b},\mathbf{r})}{d^2\mathbf{b}} =$$
$$= \langle q\bar{q}g|\left[\mathsf{S}_2(x_A,\mathbf{b},\mathbf{r}) - \mathsf{S}_3(x_A,\mathbf{b},\boldsymbol{\rho},\mathbf{r})\right]^2|q\bar{q}g\rangle =$$
$$= \langle q\bar{q}|\Sigma_A^{3\mathbb{P}}(x,x_A,\mathbf{b},\mathbf{r})|q\bar{q}\rangle, \qquad (11)$$
$$\Sigma_A^{3\mathbb{P}}(x,x_A,\mathbf{b},\mathbf{r}) =$$
$$= \log\left(\frac{x_A}{x}\right)\int d^2\boldsymbol{\rho}|\psi(\boldsymbol{\rho}) - \psi(\boldsymbol{\rho}+\mathbf{r})|^2 \times$$
$$\times\left[\mathsf{S}_2(x_A,\mathbf{b},\mathbf{r}) - \mathsf{S}_3(x_A,\mathbf{b},\boldsymbol{\rho},\mathbf{r})\right]^2.$$

Analogously, for the low-mass (LM) excitations $d\sigma_A^{LM}/d^2\mathbf{b} = \langle q\bar{q}|\Sigma_A^{LM}|q\bar{q}\rangle$ and

$$\Sigma_A^{LM}(x,x_A,\mathbf{b},\mathbf{r}) =$$
$$= \left[1-\mathsf{S}_2(x_A,\mathbf{b},\mathbf{r})\right]^2 + 2\log\left(\frac{x_A}{x}\right)\left[1-\mathsf{S}_2(x_A,\mathbf{b},\mathbf{r})\right] \times$$
$$\times\int d^2\boldsymbol{\rho}|\psi(\boldsymbol{\rho}) - \psi(\boldsymbol{\rho}+\mathbf{r})|^2 \times$$
$$\times\left[\mathsf{S}_2(x_A,\mathbf{b},\mathbf{r}) - \mathsf{S}_3(x_A,\mathbf{b},\boldsymbol{\rho},\mathbf{r})\right]. \qquad (12)$$

A fraction of DIS which is coherent diffraction, $R_{\rm coh}(x,Q^2) = \sigma_A^D(x,x_A,Q^2)/\sigma_A(x,x_A,Q^2)$, is shown in Fig.3. The large-$x$ suppression of $R_{\rm coh}(x,Q^2)$ by the nuclear form factor is evaluated with the mass spectrum [23, 24]. For the realistic dipole cross section even the lead nucleus is still a grey one: the predicted $R_{\rm coh}$ is substantially smaller than the black disc result $R_{\rm coh} = 0.5$ [4].

The total cross section of the low-mass diffraction $\sigma_A^{LM}(x,Q^2)$, i.e., DIS off the large-$\beta$ valence $q\bar{q}$ state of the pomeron, is saturated by the contribution from $M^2 \sim Q^2$. The strength of 3$\mathbb{P}$ diffraction, or DIS off the small-$\beta$ sea in the pomeron, is conveniently measured by

$$G_{3\mathbf{I\!P}}(x_{\mathbf{I\!P}}) = \frac{\partial}{\partial \xi}\int d^2\mathbf{b}\langle q\bar{q}|\Sigma_A^{3\mathbf{I\!P}}(x, x_A, \mathbf{b}, \mathbf{r})|q\bar{q}\rangle = \\ = (M^2+Q^2)\frac{d\sigma_A^{3\mathbf{I\!P}}(x_{\mathbf{I\!P}})}{dM^2}. \quad (13)$$

In Fig.4 we show the ratio $R(3\mathbf{I\!P}/LM) = G_{3\mathbf{I\!P}}(x_{\mathbf{I\!P}})/\sigma_A^{LM}(x)$, where we take $x = 10^{-3}$ and $x_{\mathbf{I\!P}} = x/\beta = 10^{-2}$, i.e., $\beta = 0.1$, where the diffractive excitation of the $q\bar{q}g$ states takes over the

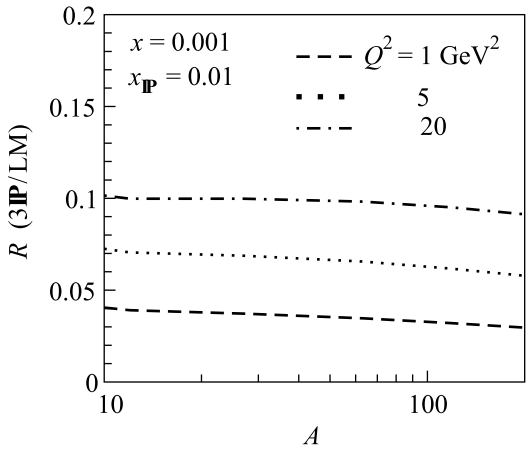


Fig.4. The predicted nuclear mass-number dependence of the ratio, $R(3\mathbf{I\!P}/LM)$, of the high-mass to low-mass diffractive DIS at several values of $Q^2$

excitation of the $q\bar{q}$ states ([23], for the experimental data see [24]). At such a value of $x_{\mathbf{I\!P}}$ the nuclear form factor effects can be neglected. The rise of $R(3\mathbf{I\!P}/LM)$ with $Q^2$ is a standard pQCD scaling violation growth of the sea parton density. Subtleties of the scaling violations at small $Q^2$ close to the nuclear saturation scale $Q_A^2$ will be discussed elsewhere.

The suppression of $R(3\mathbf{I\!P}/LM)$ for heavy nuclei, evident in Fig.4, is a unitarity effect. Indeed, the nuclear absorption in the integrand of triple-pomeron cross section, $\Sigma_A^{3\mathbf{I\!P}}(x, x_A, \mathbf{b}, \mathbf{r})$, is stronger than that of $\Sigma_A^{LM}(x, x_A, \mathbf{b}, \mathbf{r})$, and it is steadily enhanced for large $A$.

**5. Summary.** Based on the color dipole approach which correctly reproduces the experimental data on the proton structure function measured at HERA and the NMC data on nuclear shadowing, we reported the quantitative predictions for the LL$(1/x)$ evolution of the nuclear shadowing and coherent diffraction dissociation off nuclei in the kinematical range to be covered at future electron-ion colliders. We explicitly separated the contributions to both observables from the low-mass and the triple-pomeron high-mass diffractive states, including the virtual radiative correction to the low-mass diffraction. Regarding the saturation properties, even the lead nucleus is still a grey one: the fraction of DIS which is diffractive is substantially below the black disc result $R_{\rm coh} = 0.5$. The gross features of the predicted $x$ and $Q^2$ dependence of nuclear shadowing do not change much from the carbon to lead target; we also predict a suppression of the high-mass vs. low-mass coherent diffractive DIS on heavy nuclei.

This work has been partly supported by the DFG grant 436 RUS 17/82/06. VRZ acknowledges also partial support from the RFBR grant 06-02-16905-a.

## Appendix. Boundary condition for the LL$(1/x)$ evolution

The realistic input $\sigma(x_0, \mathbf{r})$ must be defined for all scales $r$, from small to non-perturbative large. Motivated by our successful BFKL-Regge color-dipole phenomenology of DIS [17, 29], at $x_0 = 0.03$ and in the limited range of $r \gtrsim 10^{-3}$ fm of the practical interest, we take

$$\sigma(x_0, r) = \sum_{i=1}^{3}\frac{\sigma_i a_i(r)}{1+a_i(r)}, \quad (14)$$

where $a_i = (r/r_0)^{2+\gamma_i}$, $r_0 = 1$ fm, $\sigma_1 = 22.5$ mb, $\sigma_2 = 20$ mb, $\sigma_3 = 8$ mb, $\gamma_1 = 0.15$,$\gamma_2 = 0.8$, $\gamma_3 = 2$. Its LL$(1/x)$ evolution is described by the Color Dipole BFKL equation [10, 11] with the infrared freezing of the one-loop, 3-flavor QCD coupling,

$$\alpha_S(q^2) = \frac{4\pi}{9\log\left[(q^2+q_f^2)/\Lambda_{QCD}^2\right]}, \quad (15)$$

where $q_f \approx 0.7$ GeV and $\Lambda_{QCD} = 0.3$ GeV. A new observation is that at the expense of somewhat smaller Debye screening radius, $R_c = 0.2$ fm vs. $R_c = 0.275$ fm in [10, 11], the LL$(1/x)$ evolution of the boundary condition (14) gives a good description of the experimental data from HERA (see Fig.5) without splitting the boundary condition into the BFKL-evolving perturbative, and non-evolving, non-perturbative, components.

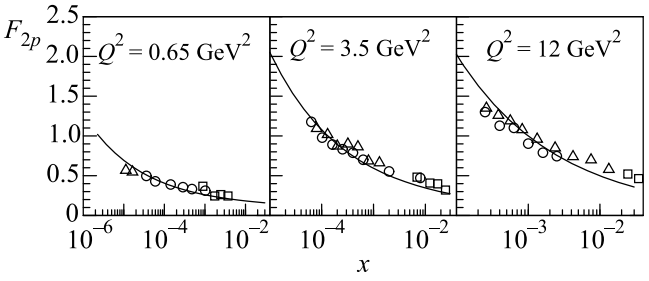


Fig.5. The proton structure function $F_{2p}(x, Q^2)$ predicted by the BFKL-evolved color dipole cross section (14) vs. the experimental data from ZEUS (open circles, [31]), H1 (triangles,[32]) and E665 (squares, [33]) Collaborations

1. N. N. Nikolaev and V. I. Zakharov, Phys. Lett. B **55**, 397 (1975); Sov. J. Nucl. Phys. **21**, 227 (1975) [Yad. Fiz. **21**, 434 (1975)].
2. I. Balitsky, Nucl. Phys. B **463**, 99 (1996); Phys. Lett. B **518**, 235 (2001); J. Jalilian-Marian, A. Kovner, A. Leonidov, and H. Weigert, Nucl. Phys. B **504**, 415 (1997); Phys Rev. D **59**, 014014 (1999); Yu. V. Kovchegov, Phys. Rev. D **60**, 034008 (1999); Phys Rev. D **61**, 074018 (2000). E. Iancu, A. Leonidov, and L. McLerran, Phys. Lett. B **510**, 133 (2001).
3. N. N. Nikolaev, W. Schäfer, B. G. Zakharov, and V. R. Zoller, J. Exp. Theor. Phys. **97**, 441 (2003) [Zh. Eksp. Teor. Fiz. **124**, 491 (2003)].
4. N. N. Nikolaev, B. G. Zakharov, and V. R. Zoller, Z. Phys. A **351**, 435 (1995).
5. M. R. Adams et al. [E665 Collaboration], Z. Phys. C **65**, 225 (1995).
6. M. S. Kugeratski, V. P. Goncalves, and F. S. Navarra, Eur. Phys. J. C **46**, 413 (2006).
7. N. N. Nikolaev and W. Schäfer, Phys. Rev. D **74**, 014023 (2006).
8. A. Deshpande, R. Milner, R. Venugopalan, and W. Vogelsang, Ann. Rev. Nucl. Part. Sci. **55**, 165 (2005), and references therein.
9. E. A. Kuraev, L. N. Lipatov, and V. S. Fadin, Sov. Phys. JETP **45**, 199 (1977) [Zh. Eksp. Teor. Fiz. **72**, 377 (1977)]; I. I. Balitsky and L. N. Lipatov Sov. J. Nucl. Phys. **28**, 822 (1978) [Yad. Fiz. **28**, 1597 (1978)].
10. N. N. Nikolaev, B. G. Zakharov, and V. R. Zoller, JETP Lett. **59**, 6 (1994) [Pisma Zh. Eksp. Teor. Fiz. **59**, 8 (1994)]; Phys. Lett. B **328**, 486 (1994).
11. N. N. Nikolaev and B. G. Zakharov, J. Exp. Theor. Phys. **78**, 598 (1994) [Zh. Eksp. Teor. Fiz. **105**, 1117 (1994)]; Z. Phys. C **64**, 631 (1994).
12. B. G. Zakharov, Phys. Atom. Nucl. **61**, 838 (1998). [Yad. Fiz. **61**, 924 (1998)].
13. N. Armesto, A. Capella, A. B. Kaidalov et al., Eur. Phys. J. C **29**, 531 (2003).
14. N. Armesto, J. Phys. G **32**, R367 (2006).
15. N. N. Nikolaev and W. Schäfer, arXiv:hep-ph/0607307.
16. J. Breitweg et al. [ZEUS Collaboration], Eur. Phys. J. C **7**, 609 (1999); C. Adloff et al. [H1 Collaboration], Phys. Lett. B **520**, 183 (2001).
17. N. N. Nikolaev, B. G. Zakharov, and V. R. Zoller, JETP Lett. **66**, 138 (1997) [Pisma Zh. Eksp. Teor. Fiz. **66**, 134 (1997)]; N. N. Nikolaev, J. Speth, and V. R. Zoller, Phys. Lett. B **473**, 157 (2000); J. Exp. Theor. Phys. **93**, 957 (2001) [Zh. Eksp. Teor. Fiz. **93**, 1104 (2001)]; Eur. Phys. J. C **22**, 637 (2002).
18. R. J. Glauber, in *Lectures in Theoretical Physics*, Vol. 1, Eds. W. E. Brittin et al., Interscience Publishers, Inc., New York, 1959, p. 315; R. J. Glauber and G. Matthiae, Nucl. Phys. B **21**, 135 (1970).
19. V. N. Gribov, Sov. Phys. JETP **29**, 483 (1969) [Zh. Eksp. Teor. Fiz. **56**, 892 (1969)].
20. N. N. Nikolaev and B. G. Zakharov, Z. Phys. C **49**, 607 (1991); V. Barone, M. Genovese, N. N. Nikolaev et al., Z. Phys. C **58**, 541 (1993).
21. B. G. Zakharov, JETP Lett. **63**, 952 (1996) [Pisma Zh. Eksp. Teor. Fiz. **63**, 906 (1996)]; ibid, **64**, 781 (1996) [Pisma Zh. Eksp. Teor. Fiz. **64**, 737 (1996)].
22. V. A. Karmanov and L. A. Kondratyuk, JETP Lett. **18**, 266 (1973) [Pisma Zh. Eksp. Teor. Fiz. **18** (1973) 451].
23. N. Nikolaev and B. G. Zakharov, Z. Phys. C **53**, 331 (1992); M. Genovese, N. N. Nikolaev, and B. G. Zakharov, J. Exp. Theor. Phys. **81**, 625 (1995) [Zh. Eksp. Teor. Fiz. **108**, 1141 (1995)]; Phys. Lett. B **380**, 213 (1996).
24. S. Chekanov et al. [ZEUS Collaboration], Nucl. Phys. B **713**, 3 (2005), and references therein.
25. H. de Vries, C.W. De Jager and C. de Vries, Atomic Data and Nuclear Data Tables **36**, 495 (1987).
26. M. Arneodo et al. [NMC Collaboration], Nucl. Phys. B **481**, 23 (1996); M. Arneodo, Phys. Rept. **240**, 301 (1994).
27. M. Arneodo et al. [NMC Collaboration], Nucl. Phys. B **441**, 12 (1995).
28. M. Arneodo et al. [NMC Collaboration], Nucl. Phys. B **481**, 3 (1996).
29. N. N. Nikolaev, W. Schäfer, B. G. Zakharov, and V. R. Zoller, JETP Letters **80**, 371 (2004) [Pisma Zh. Eksp. Teor. Fiz. **80**, 423 (2004)].
30. N. N. Nikolaev, W. Schafer, B. G. Zakharov, and V. R. Zoller, JETP Lett. **83**, 192 (2006) [Pisma Zh. Eksp. Teor. Fiz. **83**, 232 (2006)].
31. [ZEUS Collaboration], Phys. Lett. B **407**, 432 (1997); Z. f. Phys. C **69**, 607 (1996); C **72**, 399 (1996).
32. C. Adloff et al. [H1 Collaboration], Nucl. Phys. B **497**, 3 (1997); T. Ahmed et al., Nucl. Phys. B **439** (1995) 471.
33. M. R. Adams et al. [E665 Collaboration], Phys. Rev. D **54**, 3006 (1996).